

Supplementary Information

Molecular dynamics simulation of the formation mechanism of the thermal conductive filler network of polymer nanocomposites

Yue Han,^a Ke Li,^b Ziwei Li,^{*d} Jun Liu,^{*abc} Shui Hu,^b Shipeng Wen,^{abc} Li Liu,^{*abc} and
Liqun Zhang^{abc}

*a Key Laboratory of Beijing City on Preparation and Processing of Novel Polymer Materials,
Beijing University of Chemical Technology, People's Republic of China*

*b Beijing Engineering Research Center of Advanced Elastomers, Beijing University of Chemical
Technology, People's Republic of China*

*c Engineering Research Center of Elastomer Materials on Energy Conservation and Resources,
Beijing University of Chemical Technology, People's Republic of China*

*d Key Laboratory of New Processing Technology for Nonferrous Metals and Materials, Ministry
of Education, College of Materials Science and Engineering, Guilin University of Technology,
Guilin 541004, China*

* Corresponding author.

E-mail address: liziwei@glut.edu.cn (Ziwei Li), liujun@mail.buct.edu.cn (Jun Liu),
liul@mail.buct.edu.cn (Li Liu).

CONTENTS

Fig. S1 Thermal conductivity of neat polymer

Fig. S2 Thermal conduction probability of systems with NPs of $D_{NP}=2$

Fig. S3 Radial distribution function, $g_{mn}(r)$, of systems with different filler sizes at 23.8 vol%

Fig. S4 Radial distribution function, $g_{sn}(r)$, of spherical NPs around the laminar fillers

Fig. S5 Radial distribution function of hybrid-filled systems after shear

Fig. S6 Incoherent intermediate dynamic structure functions (IIDS)

Fig. S7 Structure evolution of neat polymer with chain length

Thermal conductivity of neat polymer

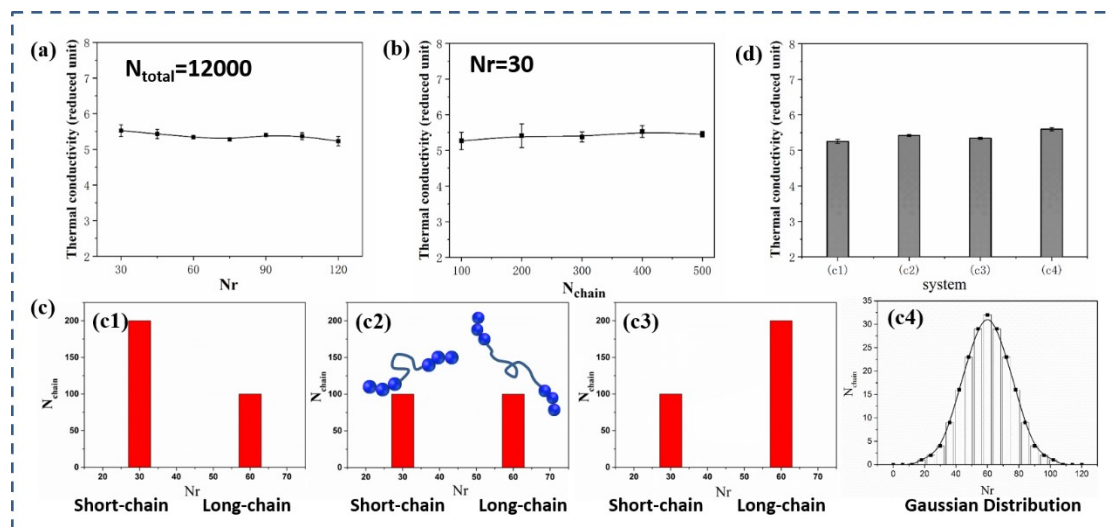


Fig. S1 Thermal conductivity of systems as a function of (a) chain length, N_r and (b) chain number (N_{chain}); (c1-c3) Chain length distribution and (c4) gaussian distribution; (d) Thermal conductivity of systems in (c1-c4).

Fig. S1(a) shows the thermal conductivity (TC), averaged by X, Y and Z directions, of polymer matrix as a function of the chain length (N_r). The total number of polymer beads in the matrix was fixed at 12,000 and N_r is set from 30σ to 120σ , corresponding to the chain number N_{chain} is from 400 to 100. The results show that TC of the system ranges from 5.0 to 6.0 (reduced unit) when N_r increases from 30σ to 120σ , which indicates that the molecular chain length has a little influence on the TC of the neat polymer. Molecular chain of $N_r=30 \sigma$ was chosen to investigate the effect of the number of polymer chains (N_{chain}) on the thermal conductivity, and the TC is almost independent of N_{chain} too. Furthermore, for practical polymeric materials, there is always a distribution of the molecular chain length. Several systems were built, which includes three chain length distribution systems (Fig. S1(c1-c3)) combined the chains of $N_r=30 \sigma$ and $N_r=60 \sigma$, and a Gaussian distribution system shown in Fig. S1(c4). Consequently, TC shown in Fig. S1(d) of these systems are similar. Finally, a system with the uniform molecular chain length of 30σ ($N_r=30$) was chosen as the matrix for it is simple and representative enough. The box dimensions of these neat polymer systems are $24.01 \pm 0.2\% \sigma$.

Thermal conduction probability of systems with NPs of $D_{NP}=2$

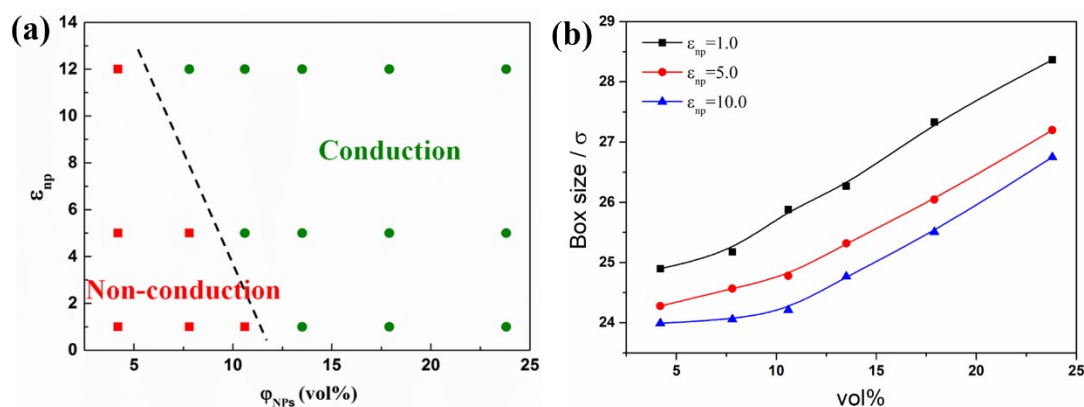


Fig. S2 (a) Phase diagram of thermal conduction probability of systems with filler size of $D_{NP}=2$ as a function of filling volume fraction. The green dot indicates that the system forms conduction, while the red dot indicates that the system fails to form conduction. (b) The box sizes of $D_{NP}=2$ systems.

The conduction probability of system with NPs of $D_{NP}=2$ is always 0 or 1, and there are almost no intermediate states because the assembly behavior is sensitive to ϵ_{np} due to the high specific surface area. NPs tend to connect to clusters as both packing fraction and physical interfacial interaction increases. The box sizes of filled systems in this work show an increase by up to 18% at most compared to neat polymer systems. Furthermore, the box size of $D_{NP}=4$ systems is similar to $D_{NP}=2$ systems, which is not list in detail.

Radial distribution function, $g_{nn}(r)$, of systems with different filler sizes at 23.8 vol%

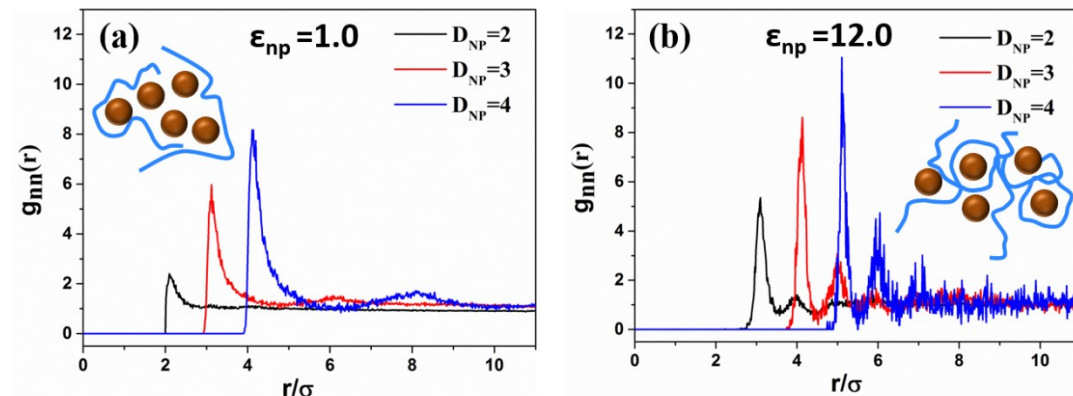


Fig. S3 Radial distribution function of filler-filler, $g_{nn}(r)$, of systems with different filler sizes at 23.8 vol%. (a) contact aggregation; (b) polymer bridging aggregation.

Fig. S3(a) shows that the maximum peak value of any system always appears at $r=(D_{NP,i}/2+D_{NP,j}/2) \sigma$, indicating that the fillers are in contact aggregation at $\epsilon_{np}=1.0$. Where $D_{NP,i}$ and $D_{NP,j}$ represent diameters of the interacting atoms i and j , respectively. While there is no contact aggregation peak in Fig. S3(b), and the maximum peak value appears at $r=(D_{NP,i}/2+D_{NP,j}/2+1) \sigma$ corresponding to the polymer bridging aggregation at $\epsilon_{np}=12.0$.

Radial distribution function, $g_{sn}(r)$, of spherical NPs around the laminar fillers

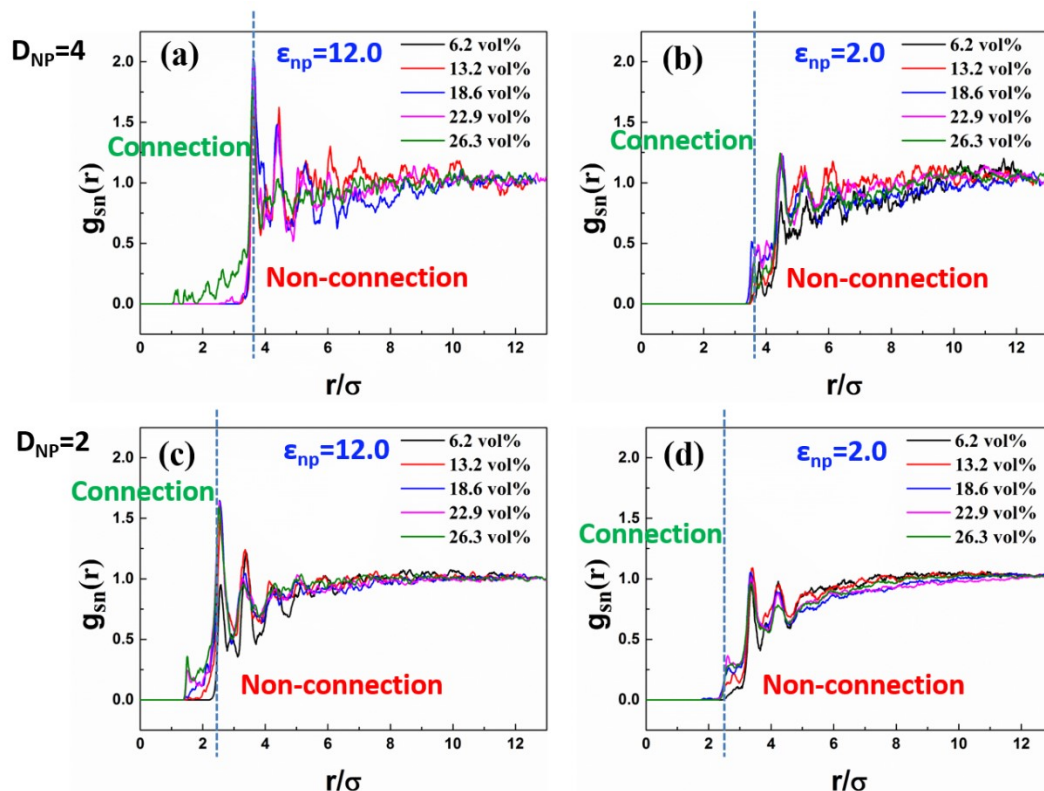


Fig. S4 Radial distribution function, $g_{sn}(r)$, of spherical NPs around the laminar fillers at different ϵ_{np} and D_{NP} . (a) $\epsilon_{np}=12.0$, $D_{NP}=4$; (b) $\epsilon_{np}=2.0$, $D_{NP}=4$; (c) $\epsilon_{np}=12.0$, $D_{NP}=2$; (d) $\epsilon_{np}=2.0$, $D_{NP}=2$.

The radial distribution function of the spherical NPs around the laminar fillers shown in Fig. S4 can qualitatively reflect the degree of overlap of the laminar/spherical filler. The vertical dotted line is the dividing line that determines whether the two fillers are in connection and form an overlapped structure. It is found that in Fig. S4 (a) and (c), a relatively large part appears at the left side of the dotted line. However, in Fig. S4 (b) and (d), only a small portion appears at the left side of the dotted line. It indicates that the strong interface of NPs-polymer ($\epsilon_{np}=12.0$) is conducive to connect the laminar fillers and spherical fillers compared to the weak interface ($\epsilon_{np}=2.0$). This is consistent with the law of the conduction probability results shown in Fig. 6(b).

Radial distribution function of hybrid-filled systems after shear

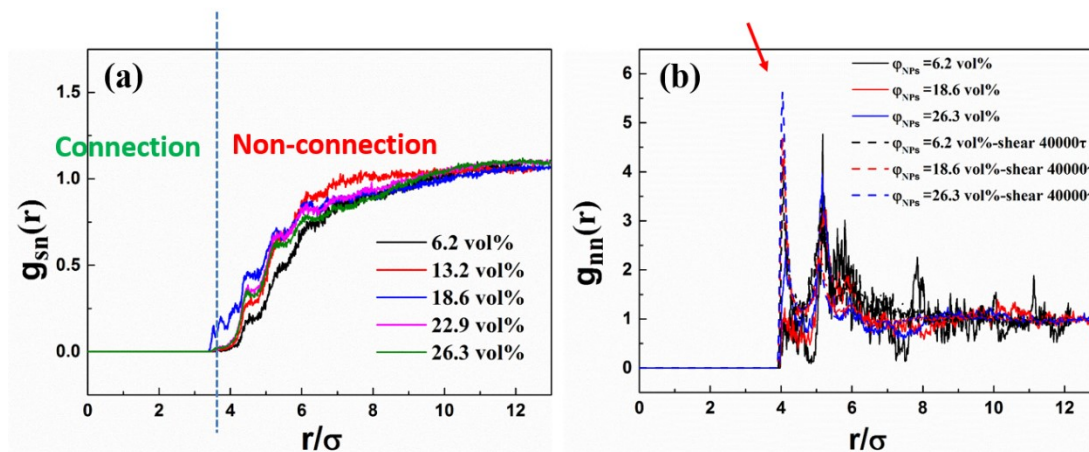


Fig. S5 (a) Radial distribution function of NPs ($D_{NP}=4$) around laminar fillers, $g_{sn}(r)$, after a shear process of 40000τ ; (b) Radial distribution function of NPs around NPs, $g_{nn}(r)$, after a shear process of 40000τ .

Fig. S5(a) shows the distribution of NPs around laminar fillers, and it is found that the content of the NPs in the connected state around laminar fillers is significantly lowered as compared with that in Fig. S4(a), which implies the separation of spherical and laminar fillers. The results of Fig. S5(b) demonstrate that the peak at $r=4\sigma$ after shear becomes significantly higher, which indicates that oscillatory shear makes more spherical fillers be in close contact with each other.

Incoherent intermediate dynamic structure functions (IIDS)

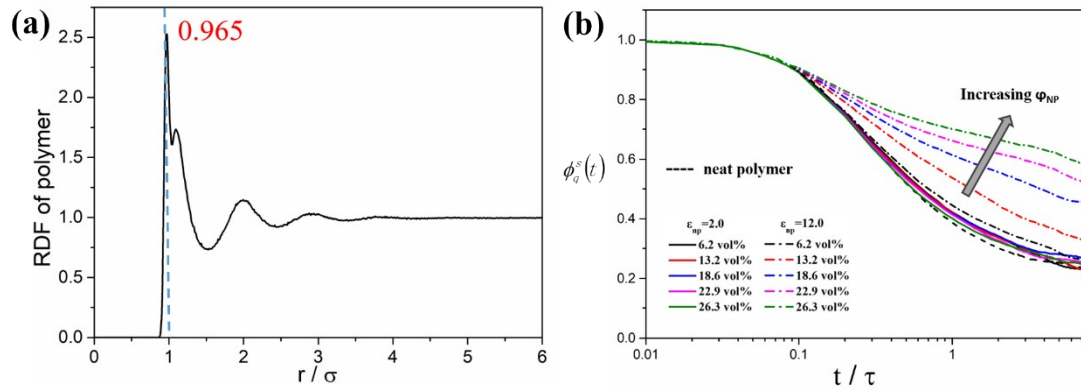


Fig. S6 (a) Radial distribution function of polymer beads; (b) Incoherent intermediate dynamic structure functions (IIDS), of polymers in $D_{NP}=4$ systems.

$$\phi_q^s(t) = \frac{1}{M} \sum_{m=1}^M \left\{ \exp \langle \mathbf{i} \mathbf{q} \cdot [\mathbf{r}_m(t) - \mathbf{r}_m(0)] \rangle \right\} = \frac{1}{M} \sum_{m=1}^M \left\{ \frac{\sin \langle q \Delta r_m(t) \rangle}{q \Delta r_m(t)} \right\}$$

We calculated the polymer scattering function, incoherent intermediate dynamic structure functions (IIDS). Where $q=2\pi/d$, d in this system is equal to 0.965, which is obtained from the position of the first peak of the radial distribution function of polymer, and therefore $q=6.51$.

Structure evolution of neat polymer with chain length

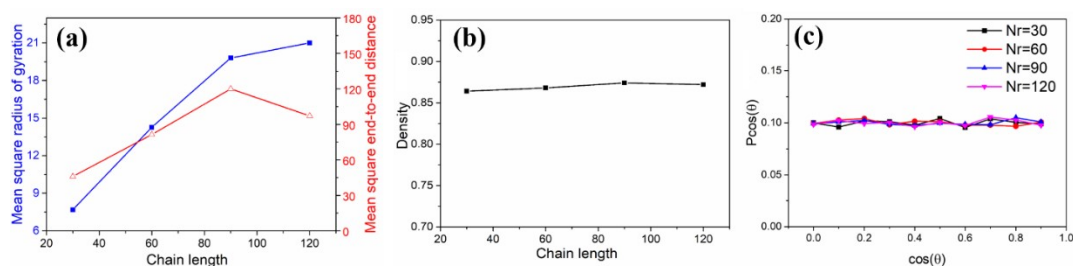


Fig. S7 (a) Mean square radius of gyration and end-to-end distance, (b) density, and (c) bond orientation distribution, of neat polymer systems.

It is generally recognized that the entanglement length N_e is 85 in “Kremer-Grest” bead-spring chains,^{1,2} which is within the chain length range that we have chosen (30 to 120). Density, mean square radius of gyration, bond orientation, and mean square end-to-end distance of polymer systems with different chain lengths are shown in Fig. S7. Though the mean square radius of gyration and mean square end-to-end distance increase as the chain length increases, the density of these systems are similar. $P\cos(\theta)$ is similar at any $\cos(\theta)$, which indicates that the probability of bond orientation angle (θ) is the same at all angles. It implies that when the chain length ranges from 30 to 120σ , the chain length does not affect the thermal conductivity, if the polymer chains are in the free entangled structure (no external force applied and no orientation).

- 1 R. S. Hoy, K. Foteinopoulou, M. Kröger. Topological analysis of polymeric melts: Chain-length effects and fast-converging estimators for entanglement length. *Phys. Rev. E.*, 2009, **80**, 031803.
- 2 J. X. Hou. Note: Determine entanglement length through monomer mean-square displacement. *J. Chem. Phys.*, 2017, **146**, 026101.